



OPEN

Microvascular and cellular dysfunctions in Alzheimer's disease: an integrative analysis perspective

Mengjie Li¹, Xiaoyan Hao¹, Zhengwei Hu¹, Jie Tian⁶, Jingjing Shi¹, Dongrui Ma¹, Mengnan Guo¹, Shuangjie Li¹, Chunyan Zuo¹, Yuanyuan Liang¹, Mibo Tang², Chengyuan Mao², Yuming Xu^{2,3,4,5} & Changhe Shi^{2,3,4,5}✉

Alzheimer's disease (AD) is the most common cause of dementia, characterized by memory loss, cognitive decline, personality changes, and various neurological symptoms. The role of blood–brain barrier (BBB) injury, extracellular matrix (ECM) abnormalities, and oligodendrocytes (ODCs) dysfunction in AD has gained increasing attention, yet the detailed pathogenesis remains elusive. This study integrates single-cell sequencing of AD patients' cerebrovascular system with a genome-wide association analysis. It aims to elucidate the associations and potential mechanisms behind pericytes injury, ECM disorder, and ODCs dysfunction in AD pathogenesis. Finally, we identified that abnormalities in the pericyte PI3K–AKT–FOXO signaling pathway may be involved in the pathogenic process of AD. This comprehensive approach sheds new light on the complex etiology of AD and opens avenues for advanced research into its pathogenesis and therapeutic strategies.

Keywords Alzheimer's disease, ScRNA-seq, GWAS, Blood–brain barrier, PI3K–AKT–FOXO

Abbreviations

AD	Alzheimer's disease
ASCs	Astrocytes
BBB	Blood–brain barrier
DOLs	Disease associated oligodendrocytes
ECM	Extracellular matrix
ECs	Endothelial cells
GLNs	Glutaminergic neurons
GSVA	Gene set variation analysis
GWAS	Genome-wide association study
MiCs	Microglia cells
NVU	Neurovascular unit
ODC	Oligodendrocyte
OPCs	Oligodendrocyte progenitor cells
scDRS	Single-cell disease relevance score
scRNA-seq	Single-cell sequencing

Alzheimer's disease (AD), the leading cause of dementia, is characterized by symptoms such as memory loss, cognitive decline, personality changes, along with other neurological manifestations including depression, restlessness, anxiety, and aggression¹. Various hypotheses have been proposed to explain the pathogenesis of AD,

¹Zhengzhou University, Zhengzhou 450000, Henan, China. ²Department of Neurology, The First Affiliated Hospital of Zhengzhou University, Zhengzhou University, 1 Jian-she East Road, Zhengzhou 450000, Henan, China. ³NHC Key Laboratory of Prevention and Treatment of Cerebrovascular Diseases, The First Affiliated Hospital of Zhengzhou University, Zhengzhou University, Zhengzhou 450000, Henan, China. ⁴Institute of Neuroscience, Zhengzhou University, Zhengzhou 450000, Henan, China. ⁵Henan Key Laboratory of Cerebrovascular Diseases, The First Affiliated Hospital of Zhengzhou University, Zhengzhou University, Zhengzhou 450000, Henan, China. ⁶Zhengzhou Railway Vocational and Technical College, Zhengzhou 450000, Henan, China. ✉email: shichanghe@zzu.edu.cn

including the amyloid-beta (A β) hypothesis², oxidative stress hypothesis³, and abnormal phosphorylation of tau proteins⁴. However, the exact pathogenic mechanisms underlying AD remain largely undefined.

Recent studies have increasingly focused on the roles of blood–brain barrier (BBB) injury^{5–9}, extracellular matrix (ECM) abnormalities^{10,11}, and oligodendrocyte (ODC) dysfunction¹² in the development of AD. The BBB, comprising pericytes, endothelial cells (ECs), astrocytes (ASCs), and the basal membrane, forms a critical component of the neurovascular unit (NVU)^{13,14}. Emerging evidence suggests that BBB damage, which can occur early in both AD patients and animal models, might contribute to AD pathogenesis independently of A β and tau accumulation^{6,15,16}. This to some extent explains the pericyte loss observed in the brains of AD patients^{17,18}. The extent of BBB impairment is closely linked to cognitive decline, highlighting the significance of pericytes in BBB integrity in AD^{19–21}. Multiple explanations exist for the cause of BBB damage, including pericytes and ECs cell degeneration, immune cell infiltration, and abnormal angiogenesis⁵. In recent years, the role of pericytes in AD has been extensively studied. Pericytes integrate the functions of ECs and ASCs to regulate BBB permeability^{13,22}. Additionally, pericytes can directly clear A β , so their loss may accelerate the progression of A β and tau pathology in AD mouse models²³. This may be related to factors such as tight junctions^{24,25} and transmembrane transport mediated by phagocytosis²⁶. The ECM, a complex network of macromolecules including collagen, elastin, fibronectin, laminin, and various glycoproteins, is vital for the structural and functional integrity of the central nervous system²⁷. Within the brain, the ECM not only supports cellular structures but also plays a pivotal role in neuronal health and signaling²⁸. It should be noted that previous studies have identified a subtype of pericytes related to the ECM, which are significantly reduced in the brain tissue of AD patients and may be associated with BBB damage in AD²⁹. ODCs are essential for myelin sheath formation and overall neuronal support. Recent research has underscored the involvement of ODCs in neurodegenerative diseases, where their dysfunction can lead to demyelination and neuronal damage^{30,31}. The discovery of disease-associated ODCs (DOLs), whose emergence is not directly linked to A β and tau pathologies^{32–35}, has opened new avenues for exploring mechanisms of AD. Studies have found that modulating the PI3K/AKT signaling pathway may alter the production and clearance of amyloid beta and tau in AD patients, thereby slowing down the disease progression³⁶. It should be noted that, due to the relatively minor proportion of the cerebral microvascular system within the brain parenchyma and the complexity inherent in research design, there have been no studies to date that conclusively illuminate the interconnections between pericyte injury, ECM disruption, and ODCs dysfunction in AD.

This study evaluated the expression of AD-related GWAS risk genes in the brain vascular system and conducted correlation analysis to infer AD-related cell subgroups. Based on this, a deeper exploration of the mechanisms was carried out, speculating on the potential process from BBB damage to ECM imbalance, and then to ODCs' functional abnormalities in AD. Additionally, the PI3K–AKT–FOXO pathway was identified as a potential mechanism leading to pericytes dysfunction.

Methods

This study used data from publicly available GEO and GWAS catalog databases. These data sources had obtained informed consent from the research participants beforehand, and according to the statements of the database providers, the collection and use of these data complied with all applicable ethical standards. Therefore, this study did not require additional ethical approval.

ScRNA-seq analysis process

We obtained the scRNA-seq data (GSE163577) (including the cortex and hippocampus) of 9 AD patients and 8 matched normal controls from the GEO public database. In this study, the research subjects were divided into two groups: the AD and the normal group. Scanpy (version 1.8.2)³⁷ was used to remove low-quality cells with more than 5% mitochondrial genes, less than 200 genes, or more than 5000 genes. BBKNN (version 1.5.1)³⁸ was used for batch effect removal in each sample. After standardization and normalization of the combined data, scanpy was used to determine the first 2000 highly variable genes in the whole data set, after which dimension reduction and clustering were successively carried out. The resolution was set to 0.3, and the principal component was set to 15. SCENIC (version 0.11.2) analysis was used for transcription factor prediction³⁹. The cell types were annotated according to the expression of marker genes: ODC (MBP), ASCs (GFAP, AQP4), pe (PDGFRB), ECs (CLDN5), MiCs (PTPRC), OPCs (DSCAM), GLNs (SYT1)²⁹. The marker genes in each cell type were calculated using the Wilcoxon test in Scanpy, and then the top 500 with the most significant *p*-values were selected as the cell-type-specific gene set. The list of marker genes is available in Supplement Table 1. Differential genes were calculated using the find markers command in Scanpy, where log2FC > 0.25 and *p* < 0.05 were considered significant.

MetaXcan identifies AD risk and protective genes

We obtained the GWAS summary data (GCST007511) from the GWAS Catalog (<https://www.ebi.ac.uk/gwas/summary-statistics>). This research included 21,982 AD patients and 41,944 controls from Europe. Detailed information can be accessed on GEO Accession viewer (GEO Accession viewer (nih.gov)). The risk and protective genes of AD were predicted by MetaXcan (version 0.6.2)⁴⁰. MetaXcan utilizes gene expression prediction models based on tissue specificity, combined with summary statistics from GWAS. It calculates the association strength between gene expression levels and phenotypes, effectively integrating information from multiple tissues and phenotypes to discover potential causal candidate genes. In this study, genes with a *z*-score greater than 2.5 were considered risk genes for AD, while genes with a *z*-score less than –2.5 were considered protective genes for AD.

ScDRS identifies disease-related cell types

The comprehensive scores of preset gene sets in single cells were calculated by single-cell disease relevance score (scDRS) (version 1.0.2)⁴¹. ScDRS is a method that associates individual cells from scRNA-seq data with disease

GWAS. It can identify cells with overexpressed disease-associated genes, thereby discovering disease-relevant cell subpopulations and mechanisms. This comprises three steps: (1) scDRS generates disease-related gene sets; (2) scDRS calculates the original disease score for each cell; (3) after gene set and cell normalization, scDRS calculates each cell's association *p*-value by comparing the cell's normalized disease-related score with the empirical distribution of the normalized control score of all gene sets and all cells.

Pathway analysis and construction gene module

Enrichr (version 3.0) was used to perform enrichment analysis of differential genes to identify gene sets associated with biological processes and pathways. Enrichr is an online tool that can perform enrichment analysis of gene lists using various reference gene set databases⁴². Details of the differential gene can be found in Supplement Tables 3–5. Gene set variation analysis (GSVA, version 1.48.3) is a method to calculate enrichment scores for a given gene set, to assess the activity level of that gene set in selected samples⁴³. Then differential analysis is performed by Wilcoxon test. We used the default parameter settings for GSVA. The STRING database (version 12.0)⁴⁴ was used to extract the protein–protein interaction network data of the differential genes. The network data from STRING were then analyzed using the iGraph package (version 1.5.1)⁴⁵ in R (version 4.2.0). A network analysis of the extracted network data employed the random walk method to highlight subnetworks or neighborhoods. We set the walk length to 3, the walk times to 1000, and the neighborhood size to 10.

Results

ScRNA-seq and GWAS summary data preprocessing

We acquired scRNA-seq data from four cortical and nine hippocampal samples collected from nine AD patients and four cortical and eight hippocampal samples from eight normal controls. After batch removal, double cell removal, low-quality cell filtering, dimension reduction, and clustering, 264,987 single cells were obtained. Display cell distribution using UMAP plots (Fig. 1A). The purpose of UMAP plots is to group similar cells together and separate different cells, so as to display cell clustering and differentiation on two-dimensional or three-dimensional graphs⁴⁶. Cell types were annotated on the basis of marker gene expression (Fig. 1C), and seven cell types were obtained: ASCs (15.5%), ECs (32.0%), glutaminergic neurons (Glns) (22.6%), microglia cells (MiCs) (4.2%), ODCs (24.1%), oligodendrocyte progenitor cells (OPCs) (1.7%), and pericytes (20.1%) (Fig. 1B). A volcano map revealed the differentially expressed genes in each cell type, and the results indicate that the top five upregulated and downregulated genes were significantly different in each cell type (Fig. 1D). These results suggest that different cell types may exhibit distinct patterns of differential gene expression and play different roles in the onset of AD.

The GWAS summary data of AD incidence included 21,982 cases and 41,944 controls. MetaXcan analysis predicted the risk and protective genes associated with AD, and yielded 125 risk genes and 120 protective genes. See Supplement Table 6 for detailed results. The genes were organized into separate gene sets to characterize their risk and protective effects on AD. These sets included known common AD risk genes such as ACE, CLU, CRI1, KAT8, HLA-DQB1, HLA-DRB1, LACTB, STX6, PLEKHA1, MTCH2, C1QTNF4, MADD, and CD2AP^{47–52}.

Identifying disease-associated cell types

ScDRS can comprehensively score a given gene set at the single-cell level to determine the overall expression of that gene set in a single cell. To explore the scores of AD risk and protective gene sets in the scRNA-seq data from AD patients, we used scDRS for evaluation and showed the outcome in UMAP, which indicated that the AD risk gene set had a high score in ODCs (Fig. 2A). The AD protective gene set was high mainly in ASCs, pericytes, and ODCs (Fig. 2B).

The marker gene sets in ODCs, ASCs, and pericytes had good specificity (Fig. 2C–E). Next, the scores of the marker gene set and AD risk and protective gene sets in cells were calculated separately prior to correlation analysis. The results show that ODCs were significantly positively correlated with AD risk (Fig. 2F), whereas there was a significant positive correlation between pericytes/ASCs and the protective effect on AD (Fig. 2G). Although the AD protective gene set was highly expressed in ODCs, its functional direction was opposite to that of pericytes/ASCs (Fig. 2G). Correlation analysis did not find any significant association with the aforementioned gene sets in other cell types. Further statistical analysis of the proportion of cells showed that ODCs increased significantly in the AD (AD group: 0.36 ± 0.12 ; normal group: 0.14 ± 0.01 , Fig. 3A), whereas pericytes decreased significantly (AD group: 0.25 ± 0.10 ; normal group: 0.13 ± 0.07 , Fig. 3B). There was no statistical difference in the proportion of ASCs between the AD and normal groups (AD group: 0.19 ± 0.07 ; normal group: 0.14 ± 0.08 , Fig. 3C). Detailed results, such as mean and standard deviation, refer to Supplement Table 7. In conclusion, by evaluating the expression of AD-related GWAS risk genes in cells, we have once again confirmed a significant association between ODCs, pericytes, ASCs, and the onset of AD from the perspective of risk genes.

To evaluate whether the above findings also exist in the hippocampus and cortex, we performed the same analysis on the hippocampus and cortex separately. The results showed that ODCs in the cortex had no significant correlation with the protective effect, while pericytes and ASCs in the hippocampus showed stronger correlation with the protective gene set (eFigure 1 in supplementary). Cell proportion analysis found that, unlike the overall analysis, the proportion of ASCs in the hippocampus of AD group increased significantly, suggesting that the proliferation of ASCs in the hippocampus of AD patients was more prominent (eFigure 2 in supplementary). In summary, the results of this study suggest that both the hippocampus and cortex are related to the pathogenesis of AD, but the hippocampus may play a more important role.

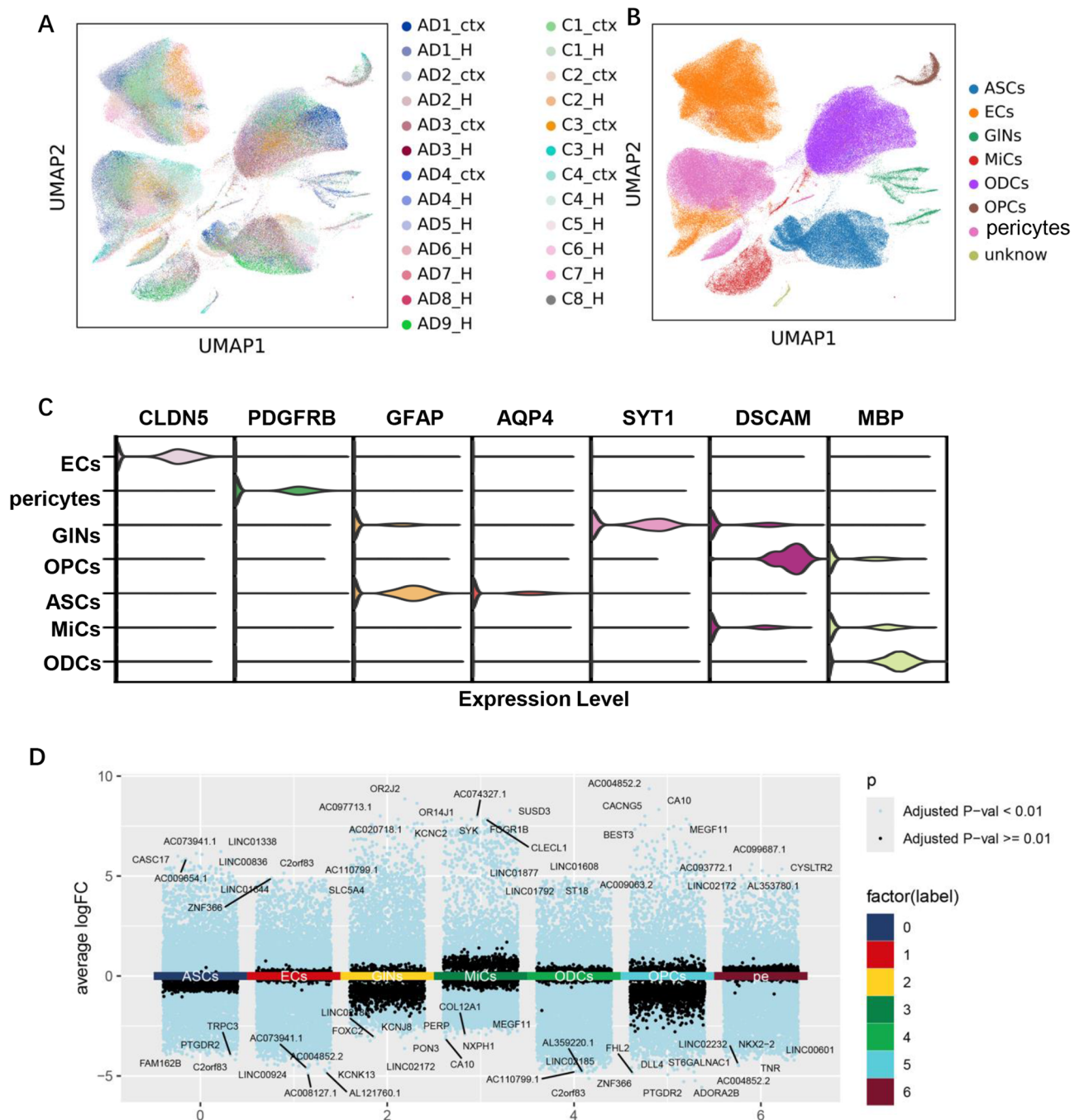


Fig. 1. (A) UMAP displaying the integration results of multiple scRNA samples with good consistency; (B) UMAP showing cell annotation results, divided into seven types: astrocytes (ASCs), endothelial cells (ECs), glutamatergic neurons (Glns), microglia cells (MiCs), oligodendrocytes (ODCs), oligodendrocyte precursor cells (OPCs), and pericytes; (C) The cell types express marker genes: ODCs (MBP), ASCs (GFAP, AQP4), pericytes (PDGFRB), ECs (CLDN5), MiCs (PTPRC), OPCs (DSCAM), and Glns (SYT1); Expression of marker genes across all cell groups; (D) Volcano plot showing the differentially expressed genes for each cell group, highlighting the top five upregulated and downregulated genes.

ECM dysregulation is involved in the pathogenesis of AD

To explore the specific pathogenesis of AD, we performed pathway enrichment analysis of total differentially expressed genes between AD and normal groups. The results show that the downregulated differentially expressed genes of AD were mainly enriched in the ECM, homeostasis, integrin cell surface interaction, and immune-related signaling pathways (Fig. 4A) that are involved in organizing extracellular structures and regulating cell proliferation and differentiation as well as cytokine response, vesicle transport, BBB transport, and other biological processes (Fig. 4B). The upregulated differentially expressed genes of AD are involved mainly in

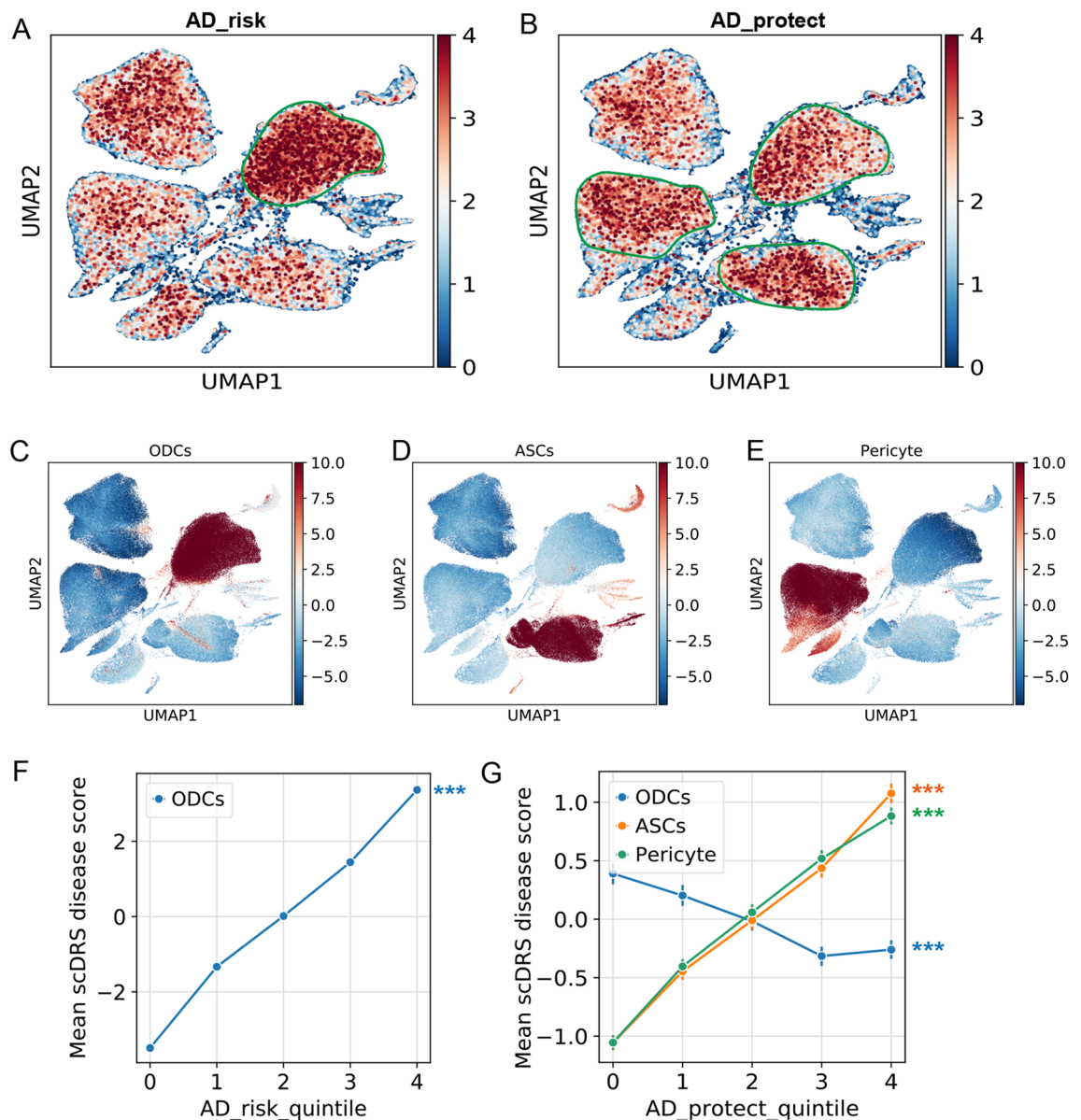


Fig. 2. ScDRS identifies disease-related cell types. **(A)** The AD risk gene set scored the highest in oligodendrocytes (ODCs); **(B)** The AD protective gene set scored higher in pericytes, astrocytes (ASCs), and ODCs; **(C)** The marker gene sets for ODCs, pericytes, and ASCs all exhibited good specificity; **(D)** Correlation analysis revealed that ODCs were positively correlated with the risk of AD; **(E)** ODCs were negatively correlated with the protective effect against AD, whereas ASCs and pericytes showed a positive correlation with the protective effect against AD. The calculation of differential genes was based on the Wilcoxon test method. The correlation analysis employed a Pearson correlation coefficient-based method to evaluate the associations between specific subgroups and various traits. This was then followed by calculating the Pearson correlation coefficient using feature scores and spatial scores, and finally, the p -value was computed by comparing this value with the Pearson correlation coefficient of the control scores. The color scale represents the scores of gene sets in the cells, transitioning from blue to red to indicate scores from low to high. ($p < 0.05$ was considered statistically significant. *** $p < 0.001$).

nervous system development and neuron projection morphogenesis (eFigure 3A,B in supplementary). The GSVA comparison analysis revealed that the activity of the ECM pathway in the AD was significantly downregulated along with the activities of adhesion, endocytosis, antigen processing and presentation, and cytokine-cytokine receptor interaction, which are involved mainly in information and substance exchange and other biological processes (Fig. 4C). We wondered whether an abnormal ECM was involved in the pathogenesis of AD and used GSVA to further explore the activation of the ECM in each cell types. The results show that the activity of the ECM pathway was significantly downregulated in all cell types (Fig. 3E), consistent with the expected results. Additionally, we conducted an analysis of ECM pathway alterations in the hippocampus and cortex separately. The results indicate that nearly all cell types in both the hippocampus and cortex of the AD group exhibit an

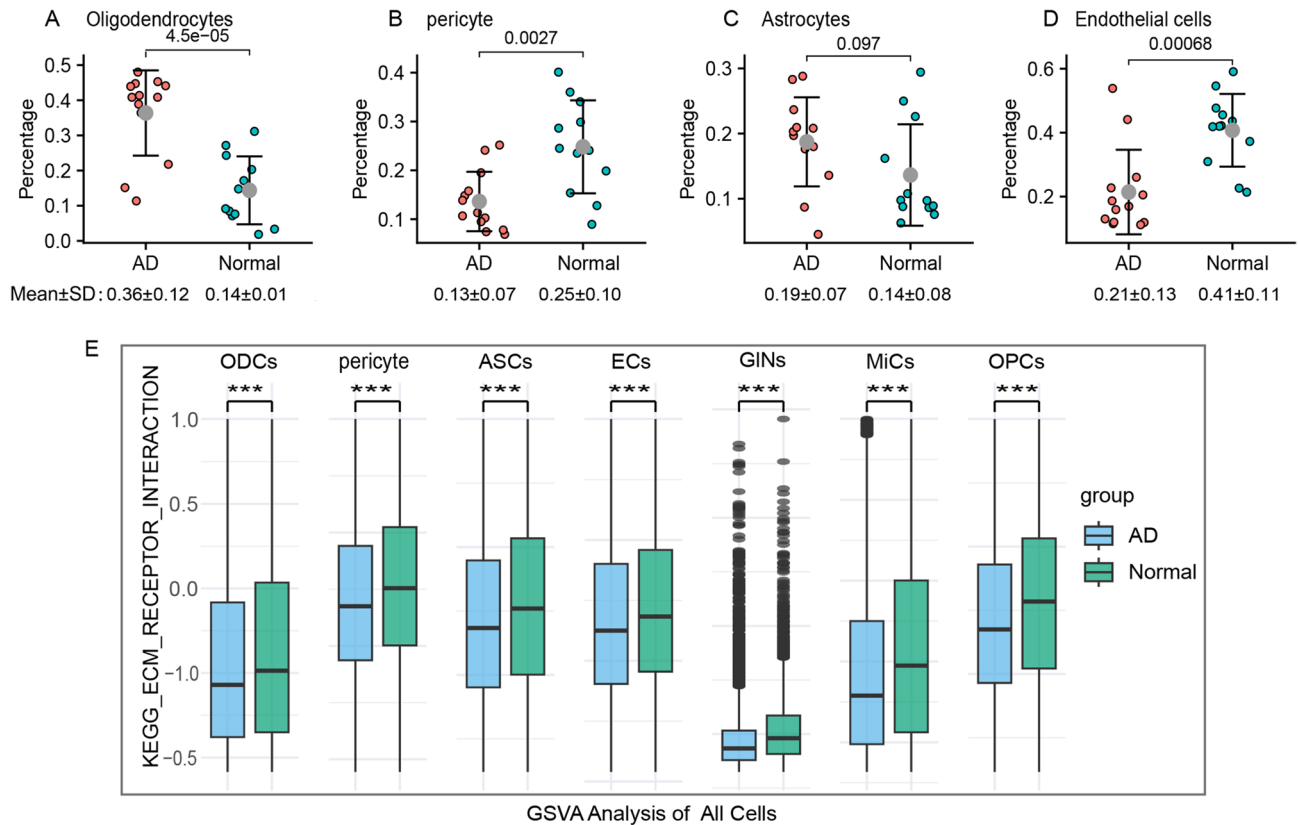


Fig. 3. Cell proportion analysis and ECM pathway enrichment analysis. **(A)** Oligodendrocytes (ODCs) increased significantly in AD; **(B,D)** Pericytes and endothelial cells (ECs) significantly decreased in AD; **(C)** There was no statistical difference in astrocytes (ASCs) between the AD and normal groups. Each point in the scatter plot represents an individual sample. Statistical significance was determined using the t-test. The annotations in the figure represent the mean value plus or minus one standard deviation, indicating the range of variation around each data point, and are labeled below each graph. **(E)** Gene Set Variation Analysis (GSEA) showed that ECM pathway activity in AD was significantly downregulated in all cell types. Wilcoxon test. The upper and lower boundaries of the boxplot represent the upper quartile (Q3) and lower quartile (Q1) of the data, respectively. The horizontal line inside the box represents the median (Q2). (***) $p < 0.001$.

imbalance in the ECM, with the hippocampus showing more pronounced effects (eFigure 2I,J in supplementary). In conclusion, an abnormal ECM pathway may be a cause of AD pathogenesis.

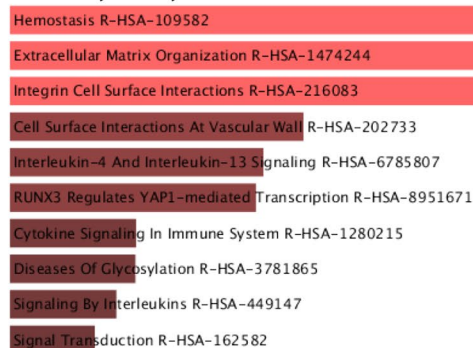
ODC hyperplasia and dysfunction caused by an abnormal ECM

To explore the role of ODCs in the pathogenesis of AD, pathway enrichment analysis was conducted on ODCs' differentially expressed genes, and the results show that the downregulated differentially expressed genes of AD were enriched mainly in the ECM, adhesion, tight junction, MAPK, and other pathways (Fig. 5A). It is involved in biological processes such as extracellular structure organization, response to cytokine, vesicle transport, and the regulation of ECs migration (Fig. 5B). The upregulated differentially expressed genes of AD are involved mainly in nervous system development, axonogenesis, and the regulation of neuron death (eFigure 3C,D in supplementary). GSEA was further used to evaluate differences in the activity of pathways in ODCs between the AD and normal groups, and the results show that the activity of the ECM pathway in the AD was significantly downregulated as was the activity of pathways associated with adhesion, cytokine–cytokine receptor interaction, and the MAPK pathway. To better display the differential results, we use t-value to draw box plots to show the enrichment level of pathways (Fig. 5C). Overall, we speculate that ODC dysfunction caused by an abnormal ECM pathway may be a pathogenic mechanism of AD.

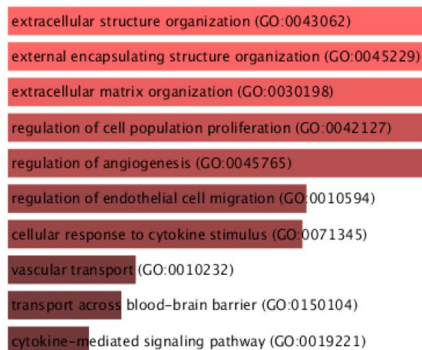
Pericyte disorders and BBB injury lead to ECM dysregulation in AD

To explore the possible causes of ECM imbalance in AD, we performed pathway enrichment analysis of pericytes' differentially expressed genes, and the results show that the downregulated differentially expressed genes of AD were enriched mainly in the PI3K–AKT, VEGF, and adhesion pathways (Fig. 6A) and were involved in biological processes such as BBB transport, vesicle transport, ECM organization, and cytokine response (Fig. 6B). The upregulated differentially expressed genes of AD are involved mainly in myelin development, axon protein localization, ODC differentiation, and other biological processes (supplement Fig. 1E/F). Further GSEA comparative analysis showed that the activity of the PI3K–AKT pathway was significantly downregulated in the AD along with the activities of the FOXO, cell cycle, VEGF, cytokine–cytokine receptor interaction, and MAPK

A Pathway Analysis



B Biological Process



C GSVA Analysis

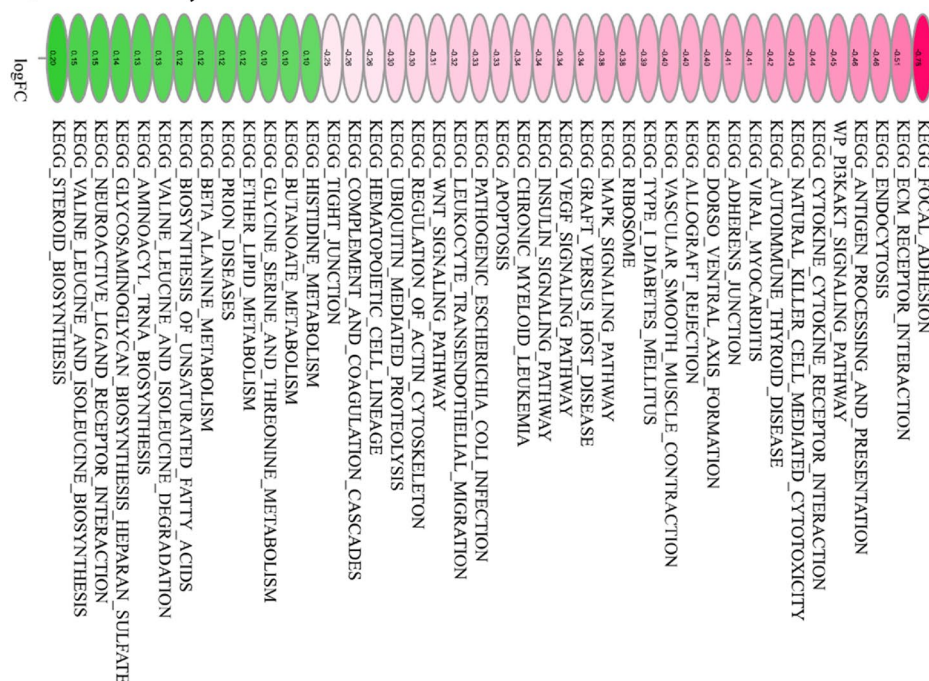
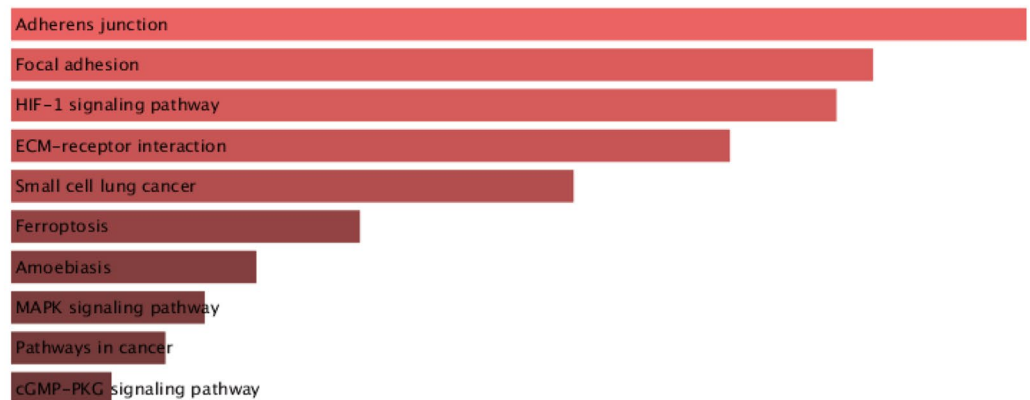


Fig. 4. Pathway analysis of downregulated differential genes in AD. (A) Pathway enrichment analysis showed an abnormal ECM pathway in AD; (B) Biological process analysis indicated abnormalities in the ECM, vascular transport, and angiogenesis in AD. (C) GSVA analysis showed that the ECM was significantly downregulated in AD. ($p < 0.05$ was considered statistically significant.)

pathways (Fig. 6C). Modules were constructed for the differentially expressed genes in downregulated pathways in GSVA, and the PI3K–AKT pathway was found to be in the central position (Fig. 7A). It should be noted that

A Pathway Analysis



B Biological Process

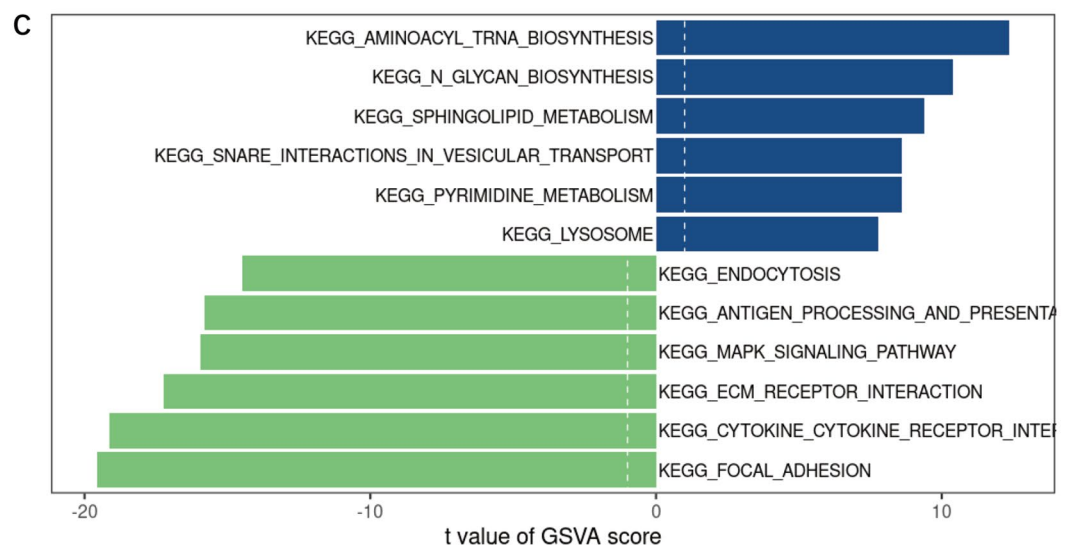
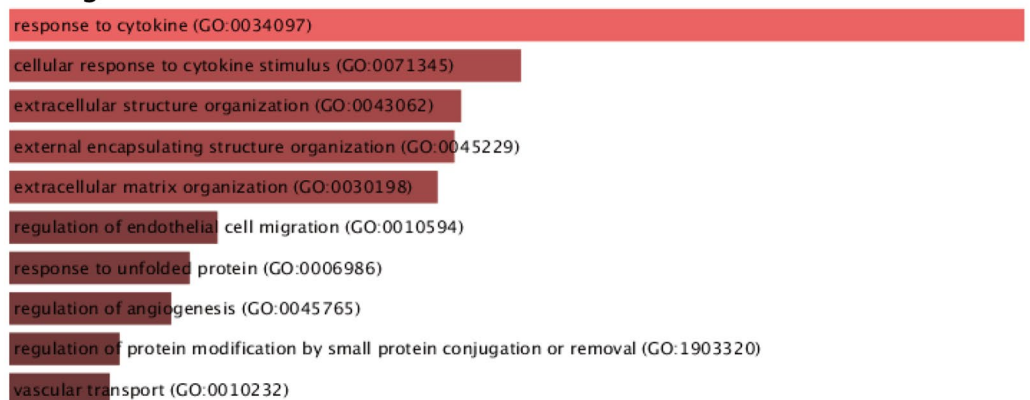
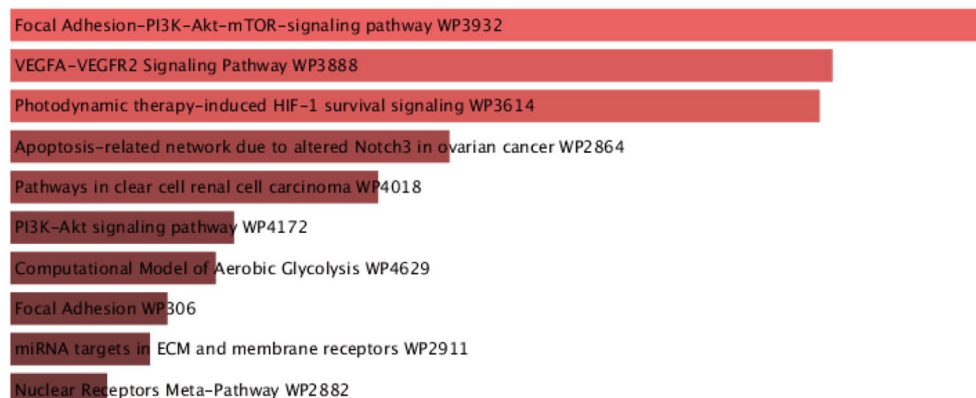


Fig. 5. Differential gene pathway enrichment analysis. (A/B) Pathway and biological process enrichment analysis revealed that downregulated genes in ODCs were enriched in pathways such as the ECM, vascular transport, response to unfold protein, ferroptosis, and angiogenesis; (C) GSVA showed that ECM pathway activity was significantly downregulated in AD. Bar chart display the distribution of t-values across samples for different gene sets, used to assess their enrichment in various samples. Higher t-values indicate more significant enrichment. ($p < 0.05$ was considered statistically significant.)

A Pathway Analysis



B Biological Process

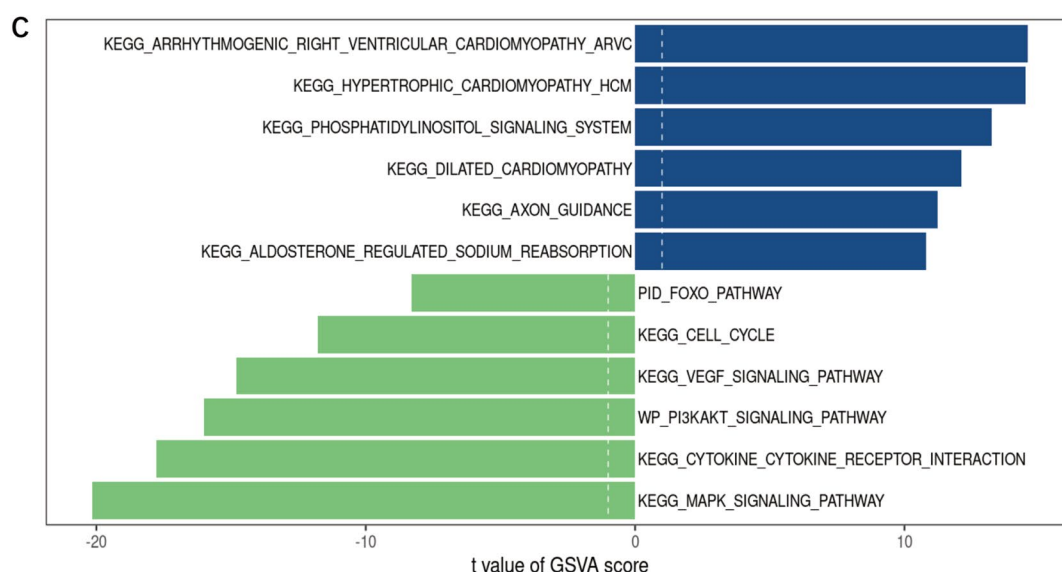
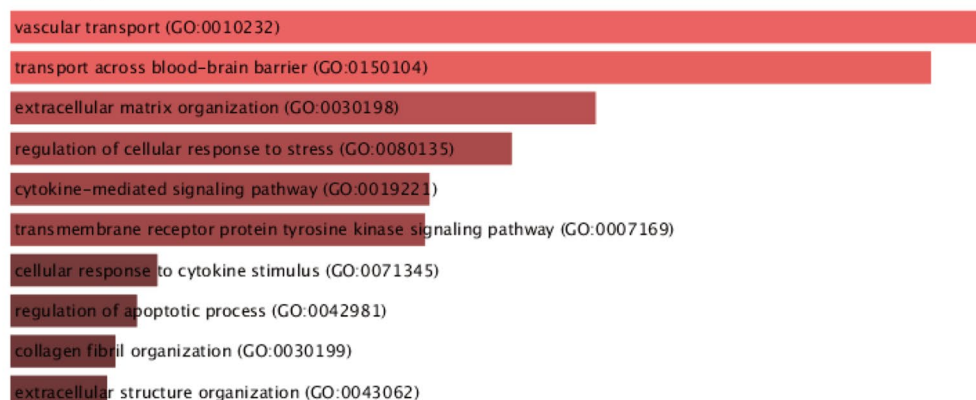


Fig. 6. Differential gene pathway analysis. (A) Pathway enrichment analysis showed that pericytes' downregulated genes in AD were enriched in the PI3K-AKT pathway; (B) Enrichment analysis for downregulated genes primarily identifies significant enrichment in pathways associated with vascular transport, transport across the blood-brain barrier (BBB), and the extracellular matrix (ECM). (C) GSEA showed that PI3K-AKT pathway activity was significantly downregulated in pericytes of AD.

abnormalities in the PI3K-AKT pathway are not evident in other cell types (not shown). In conclusion, we speculate that an abnormal PI3K-AKT pathway may be a pathogenic pathway for pericyte dysfunction in AD.

The PI3K–AKT pathway is involved in cell development, metabolism, proliferation, survival, and angiogenesis, and phosphorylated AKT (p-AKT) plays a key role in regulating the activity of the pathway. PI3K activates the PI3K–AKT pathway by binding to the phosphatidylinositol-dependent kinase (PDK) family to induce AKT to the cell membrane for phosphorylation^{53,54}. In further exploring the specific mechanism of the abnormal PI3K–AKT pathway in the pericytes of AD, we found that the expression of PDK1/3/4 in the pericytes of the AD was significantly downregulated (Fig. 7B). The expression levels of genes inhibiting AKT dephosphorylation, such as PPP2R1B and PPP2R2D, were also significantly downregulated (Fig. 7B), which decreased the p-AKT level and inhibited the PI3K–AKT pathway. The FOXO family is the downstream regulator of AKT. A SCENIC analysis found that pericytes FOXO1/4/6 transcription factor activity was significantly upregulated in the AD (Fig. 7C). The schematic diagram of the mechanism is shown in Fig. 7D. These results indicate that an abnormal PI3K–AKT–FOXO pathway of pericyte may be a pathogenic cause of AD.

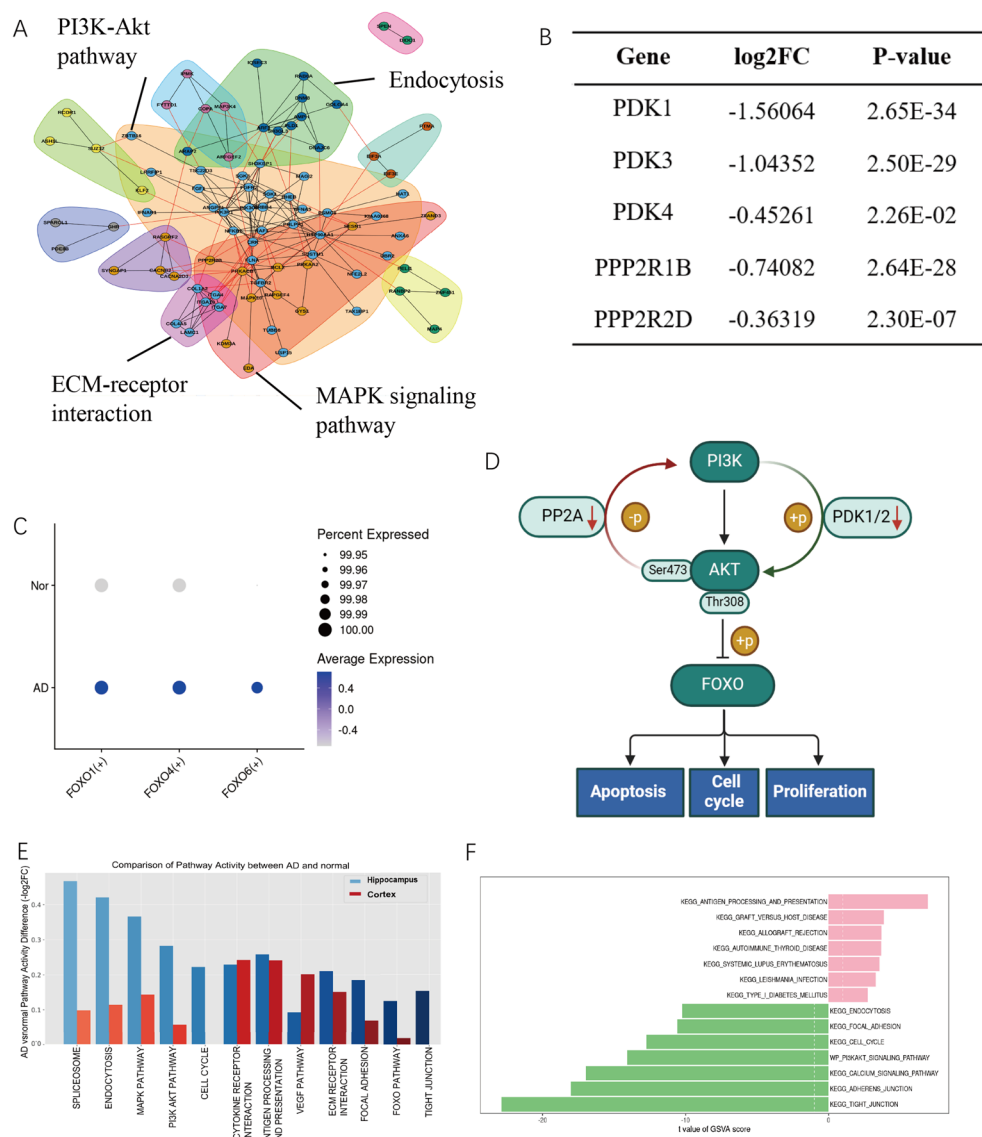


Fig. 7. (A) The PI3K–AKT pathway was central in the construction of the pericytes differential gene module; (B) Key genes related to the PI3K–AKT pathway were significantly downregulated in the pericytes of AD patients; (C) SCENIC transcription factor prediction analysis showed that the activity of FOXO1/4/6 was significantly upregulated in the pericytes of AD; (D) Schematic diagram of the PI3K–AKT–FOXO pathway; (–p: dephosphorylation process; +p: phosphorylation process) (E) GSVA analysis of hippocampal and cortical pericytes revealed differences in pathway activity between the AD and normal groups; (F) GSVA analysis indicated that hippocampal immune-related pathway activity in AD was significantly higher than in the cortex, whereas the activity levels of the PI3K–AKT, FOXO, and cell cycle pathways were significantly lower than those in the cortex. ($p < 0.05$ was considered statistically significant.)

Hippocampal pericyte damage and immune infiltration are more significant in AD

Given that hippocampal atrophy is a typical pathological feature of AD⁵⁵, we wondered whether we would find different pathological mechanisms between the hippocampal and cortical pericyte samples in AD. Therefore, we conducted a comparative GSEA analysis of the hippocampal and cortical pericytes of the AD and normal groups. We found that the activities of the cytokine–cytokine receptor interaction, antigen processing and presentation, ECM, and other pathways in the hippocampus and cortex were significantly downregulated. Most of the key pathways, such as the PI3K–AKT, FOXO, endocytosis, and spliceosome pathway, were more significantly downregulated in the hippocampus (Fig. 7E). We further compared differences in the activation levels of pericyte pathways in the hippocampal and cortical regions of AD patients by GSEA and found that the activities of the PI3K–AKT pathway, endocytosis pathway, tight junction pathway, and adhesion pathway were significantly decreased in the pericytes of AD patients, whereas immune-related signaling pathways, such as the antigen processing and presentation, and autoimmune were significantly activated (Fig. 7F). These findings suggest that AD patients have more significant pericyte damage and immune levels in the hippocampus.

Abnormal ECs are involved in the disruption of BBB function in AD

Although scDRS did not find a significant association between ECs and AD, given their important role in the BBB and their significant reduction in AD (Fig. 3D and eFigure 2D,H in supplementary), it suggests that ECs may be involved in BBB damage in AD. The cell proportion analysis results are as follows: AD group: 0.21 ± 0.13 ; normal group: 0.41 ± 0.1 . Interestingly, although the GSEA results showed a significant downregulation of pathways such as tight junction, focal adhesion, adherens junction, and endocytosis in the hippocampal region of the AD group, they showed a significant activation of pathways such as tight junction, adherens junction, and endocytosis (only including ECs) in the cortical (eFigure 4 in supplementary), which are essential for the BBB barrier and transport functions of pericytes and endothelial cells^{56,57}. In summary, these results suggest that the BBB in the hippocampal of AD may suffer more severe damage than in the cortex.

Discussion

Sn-RNA approaches help reveal molecular disturbances in AD, but most of these studies focus on abundant brain cell types^{58–60}. Previous research has already identified significant associations between gene expression patterns of different cell types and AD risk genes, including ECs, pericytes, ASCs, and MiCs^{51,61–63}. Luquez et al. and Murdock et al. have provided detailed summaries of gene expression patterns and potential pathogenic processes in different cell types in AD^{64,65}. Similarly, our study utilized scDRS to assess the expression of AD risk genes in the brain vascular single-cell atlas and conducted correlation analysis, identifying cell types significantly associated with AD risk genes, including ODCs, pericytes, and ASCs. In contrast to the expression-weighted cell type enrichment (EWCE) approach commonly used in previous studies, which analyzes associations between specific risk genes and cell types, scDRS implements a comprehensive weighting strategy for all genes in individual cells, providing a better assessment of the cumulative risk level of each cell in multi-gene diseases. First, we found that the PI3K–AKT–FOXO pathway is a potential mechanism for pericyte damage⁶⁶, which can lead to BBB disruption and further result in ECM imbalance^{10,11} and immune infiltration^{67,68}. Our results partially explain how the PI3K/AKT signaling pathway may alter the production and clearance of amyloid beta and tau in AD patients, thereby slowing down disease progression³⁶. Additionally, our results show that the downregulation of the pericyte FOXO pathway, specifically the downregulation of p-AKT, activated the transcriptional regulatory activity of the downstream FOXO family and inhibited FOXO. The FOXO pathway is involved in regulating cell proliferation, and its activation can promote cell apoptosis and inhibit the cell cycle⁶⁹. Finally, we observed that pericytes in the hippocampal region of AD patients exhibit more severe functional impairment and immune infiltration compared to those in the cortical region. This supports the notion that AD may be an autoimmune disease^{67,68}.

Although previous studies have revealed the selective susceptibility of pericytes in AD, which is also confirmed by our results, their explanations often focus on describing risk genes and lack deeper insights. However, we found that an abnormal PI3K–AKT–FOXO pathway may be the underlying cause of pericytes injury in AD. Additionally, several explanations are offered for the loss of pericytes in AD patients, such as PDGFR β ⁷⁰ and PI3K β ⁷¹ signal loss as well as APOE-mediated activation of cyclophilin A (CypA) and matrix metalloproteinase-9 (MMP9)⁷. Pericytes also play a role in regulating blood flow. The dysfunction and decrease of pericytes reduce the regulating effect of pericytes on cerebral blood flow, offering a possible explanation for the decreased cerebral blood flow in AD patients⁷².

Our results show that there is a severe imbalance in the ECM and activation of immune responses in the brains of patients with AD. As an important part of the extracellular environment, the ECM is involved in the morphological and structural support of cells and the survival, differentiation, development, and migration of nerve cells. It has been shown to be highly related to the immune system, and its disorder is the direct or indirect cause of most chronic diseases^{73–75}. AD risk genes are all important components of the ECM, such as *ADAMTS1*, *ADAMTS4*, *FERMT2*, and *AGRN*⁶¹. Additionally, it has been proved that disorders of HA, heparin sulfate proteoglycan (HSPG), chondroitin sulfate proteoglycan (CSPG), and other ECMs are closely related to the onset of AD and are associated with damage to the BBB^{74,76–78}. Although previous studies identified a subtype of pericytes related to the ECM and associated with BBB damage, we found that ECM imbalance occurs in all cell types, not specifically in pericytes. We believe this is likely a consequence rather than the cause of BBB damage²⁹.

We found that AD risk genes are highly expressed in ODCs, suggesting that ODCs are involved in the pathogenesis of AD. We observed ECM imbalance in ODCs in AD patients, accompanied by downregulation of pathways involved in vesicle transport and ECs migration regulation, and upregulation of pathways regulating neuronal death. ODCs, as myelin-forming cells, are protective of neurons and can be sensitive to and respond to

changes in the external environment. Recent studies have identified a class of DOLs in postmortem examinations of AD patients and animal models whose cell biosynthesis and lipid processing are enhanced and whose numbers increase significantly with disease progression^{33,59}. The proliferation of DOLs can be induced in abnormal microenvironments, such as those affected by immune inflammation, cytokines, and damage-related molecular patterns³⁵, which further demonstrates the importance of the ECM's homeostasis of ODCs to maintain its normal function and to some extent explains the proliferation of ODCs. Given the substantial evidence suggesting that BBB damage may be the initiating factor in AD^{5,6,15,16,18,23,79}, we speculate that the ECM mediates BBB damage leading to the dysfunction of ODCs.

However, it's important to address its limitations for a comprehensive understanding. Although sc-RNA studies have provided unprecedented resolution for investigating cellular vulnerability in AD, significant questions remain about how neurons become dysregulated and how interactions between various cell types shape their vulnerability or resistance in the disease. Moreover, the selective vulnerability of cell types may vary across different studies, making it necessary to perform comprehensive reanalysis of multiple datasets. While these tools are powerful for hypothesis generation and preliminary analysis, more direct evidence may be needed. This approach, while useful for understanding broader mechanistic themes, may overlook critical nuances at the molecular or cellular level that could be pivotal in AD pathology. The complexity of neurodegenerative diseases like AD often requires a multi-dimensional analysis that goes beyond pathway-level insights to include gene expression profiles, protein interactions, and possibly even epigenetic factors. To address these limitations, subsequent research should aim to incorporate experimental validation of key findings, particularly those related to protein molecules implicated in AD. This could involve in vitro studies using cell lines or patient-derived cells, as well as in vivo studies in animal models. Such experimental approaches would provide a more solid foundation for the bioinformatic predictions and help translate these findings into practical clinical applications.

Conclusion

This study revealed the association and potential pathogenesis of BBB injury, ECM disorder, and ODCs dysfunction in the pathogenesis of AD, providing an important direction for further exploration of the pathogenesis and treatment of AD.

Data availability

The singlecell dataset generated and/or analyzed during the current study is available in the GEO repository, GSE163577 (<https://www.ncbi.nlm.nih.gov/geo/query/acc.cgi?acc=GSE163577>). The GWAS summary data generated and/or analyzed during the current study is available in the GWAS Catalog, GCST007511 (<https://www.ebi.ac.uk/gwas/summary-statistics>).

Received: 8 May 2024; Accepted: 2 September 2024

Published online: 09 September 2024

References

- Scheltens, P. *et al.* Alzheimer's disease. *Lancet* **397**, 1577–1590. [https://doi.org/10.1016/s0140-6736\(20\)32205-4](https://doi.org/10.1016/s0140-6736(20)32205-4) (2021).
- Hardy, J. & Selkoe, D. J. The amyloid hypothesis of Alzheimer's disease: Progress and problems on the road to therapeutics. *Science* **297**, 353–356. <https://doi.org/10.1126/science.1072994> (2002).
- Maccioni, R. B., Farias, G., Morales, I. & Navarrete, L. The revitalized tau hypothesis on Alzheimer's disease. *Arch. Med. Res.* **41**, 226–231. <https://doi.org/10.1016/j.arcmed.2010.03.007> (2010).
- Terry, A. V. Jr. & Buccafusco, J. J. The cholinergic hypothesis of age and Alzheimer's disease-related cognitive deficits: Recent challenges and their implications for novel drug development. *J. Pharmacol. Exp. Ther.* **306**, 821–827. <https://doi.org/10.1124/jpet.102.041616> (2003).
- Sweeney, M. D., Sagare, A. P. & Zlokovic, B. V. Blood–brain barrier breakdown in Alzheimer disease and other neurodegenerative disorders. *Nat. Rev. Neurol.* **14**, 133–150. <https://doi.org/10.1038/nrneurol.2017.188> (2018).
- Zhao, Z., Nelson, A. R., Betsholtz, C. & Zlokovic, B. V. Establishment and dysfunction of the blood–brain barrier. *Cell* **163**, 1064–1078. <https://doi.org/10.1016/j.cell.2015.10.067> (2015).
- Ishii, M. & Iadecola, C. Risk factor for Alzheimer's disease breaks the blood–brain barrier. *Nature* **581**, 31–32. <https://doi.org/10.1038/d41586-020-01152-8> (2020).
- Sweeney, M. D., Zhao, Z., Montagne, A., Nelson, A. R. & Zlokovic, B. V. Blood–brain barrier: From physiology to disease and back. *Physiol. Rev.* **99**, 21–78. <https://doi.org/10.1152/physrev.00050.2017> (2019).
- Wang, D. *et al.* Relationship between amyloid- β deposition and blood–brain barrier dysfunction in Alzheimer's disease. *Front. Cell Neurosci.* **15**, 695479. <https://doi.org/10.3389/fncel.2021.695479> (2021).
- Lepelletier, F. X., Mann, D. M., Robinson, A. C., Pinteaux, E. & Boutin, H. Early changes in extracellular matrix in Alzheimer's disease. *Neuropathol. Appl. Neurobiol.* **43**, 167–182. <https://doi.org/10.1111/nan.12295> (2017).
- Sun, Y. *et al.* Role of the extracellular matrix in Alzheimer's disease. *Front. Aging Neurosci.* **13**, 707466. <https://doi.org/10.3389/fnagi.2021.707466> (2021).
- Chen, W. T. *et al.* Spatial transcriptomics and in situ sequencing to study Alzheimer's disease. *Cell* **182**, 976–991.e919. <https://doi.org/10.1016/j.cell.2020.06.038> (2020).
- Armulik, A. *et al.* Pericytes regulate the blood–brain barrier. *Nature* **468**, 557–561. <https://doi.org/10.1038/nature09522> (2010).
- Sweeney, M. D., Ayyadurai, S. & Zlokovic, B. V. Pericytes of the neurovascular unit: Key functions and signaling pathways. *Nat. Neurosci.* **19**, 771–783. <https://doi.org/10.1038/nn.4288> (2016).
- Lin, Z. *et al.* Blood–brain barrier breakdown in relationship to Alzheimer and vascular disease. *Ann. Neurol.* **90**, 227–238. <https://doi.org/10.1002/ana.26134> (2021).
- Halliday, M. R. *et al.* Accelerated pericyte degeneration and blood–brain barrier breakdown in apolipoprotein E4 carriers with Alzheimer's disease. *J. Cereb. Blood Flow Metab.* **36**, 216–227. <https://doi.org/10.1038/jcbfm.2015.44> (2016).
- Sengillo, J. D. *et al.* Deficiency in mural vascular cells coincides with blood–brain barrier disruption in Alzheimer's disease. *Brain Pathol.* **23**, 303–310. <https://doi.org/10.1111/bpa.12004> (2013).

18. Miners, J. S., Schulz, I. & Love, S. Differing associations between A β accumulation, hypoperfusion, blood–brain barrier dysfunction and loss of PDGFRB pericyte marker in the precuneus and parietal white matter in Alzheimer's disease. *J. Cereb. Blood Flow Metab.* **38**, 103–115. <https://doi.org/10.1177/0271678x17690761> (2018).
19. Montagne, A. *et al.* APOE4 leads to blood–brain barrier dysfunction predicting cognitive decline. *Nature* **581**, 71–76. <https://doi.org/10.1038/s41586-020-2247-3> (2020).
20. Nikolakopoulou, A. M. *et al.* Pericyte loss leads to circulatory failure and pleiotrophin depletion causing neuron loss. *Nat. Neurosci.* **22**, 1089–1098. <https://doi.org/10.1038/s41593-019-0434-z> (2019).
21. Winkler, E. A., Sagare, A. P. & Zlokovic, B. V. The pericyte: A forgotten cell type with important implications for Alzheimer's disease? *Brain Pathol.* **24**, 371–386. <https://doi.org/10.1111/bpa.12152> (2014).
22. Daneman, R., Zhou, L., Kebede, A. A. & Barres, B. A. Pericytes are required for blood–brain barrier integrity during embryogenesis. *Nature* **468**, 562–566. <https://doi.org/10.1038/nature09513> (2010).
23. Sagare, A. P. *et al.* Pericyte loss influences Alzheimer-like neurodegeneration in mice. *Nat. Commun.* **4**, 2932. <https://doi.org/10.1038/ncomms3932> (2013).
24. Hartz, A. M. *et al.* Amyloid- β contributes to blood–brain barrier leakage in transgenic human amyloid precursor protein mice and in humans with cerebral amyloid angiopathy. *Stroke* **43**, 514–523. <https://doi.org/10.1161/strokeaha.111.627562> (2012).
25. Cockerill, I., Oliver, J. A., Xu, H., Fu, B. M. & Zhu, D. Blood–brain barrier integrity and clearance of amyloid- β from the BBB. *Adv. Exp. Med. Biol.* **1097**, 261–278. https://doi.org/10.1007/978-3-319-96445-4_14 (2018).
26. Ayloo, S. *et al.* Pericyte-to-endothelial cell signaling via vitronectin-integrin regulates blood–CNS barrier. *Neuron* **110**, 1641–1655. <https://doi.org/10.1016/j.neuron.2022.02.017> (2022).
27. Frantz, C., Stewart, K. M. & Weaver, V. M. The extracellular matrix at a glance. *J. Cell Sci.* **123**, 4195–4200. <https://doi.org/10.1242/jcs.023820> (2010).
28. Testa, D., Prochiantz, A. & Di Nardo, A. A. Perineuronal nets in brain physiology and disease. *Semin. Cell Dev. Biol.* **89**, 125–135. <https://doi.org/10.1016/j.semcdb.2018.09.011> (2019).
29. Yang, A. C. *et al.* A human brain vascular atlas reveals diverse mediators of Alzheimer's risk. *Nature* **603**, 885–892. <https://doi.org/10.1038/s41586-021-04369-3> (2022).
30. Behrendt, G. *et al.* Dynamic changes in myelin aberrations and oligodendrocyte generation in chronic amyloidosis in mice and men. *Glia* **61**, 273–286. <https://doi.org/10.1002/glia.22432> (2013).
31. Nasrabady, S. E., Rizvi, B., Goldman, J. E. & Brickman, A. M. White matter changes in Alzheimer's disease: A focus on myelin and oligodendrocytes. *Acta Neuropathol. Commun.* **6**, 22. <https://doi.org/10.1186/s40478-018-0515-3> (2018).
32. Zhang, X. *et al.* Oligodendroglial glycolytic stress triggers inflammasome activation and neuropathology in Alzheimer's disease. *Sci. Adv.* **6**, abb8680. <https://doi.org/10.1126/sciadv.abb8680> (2020).
33. Pandey, S. *et al.* Disease-associated oligodendrocyte responses across neurodegenerative diseases. *Cell Rep.* **40**, 111189. <https://doi.org/10.1016/j.celrep.2022.111189> (2022).
34. Sadick, J. S. *et al.* Astrocytes and oligodendrocytes undergo subtype-specific transcriptional changes in Alzheimer's disease. *Neuron* **110**, 1788–1805. <https://doi.org/10.1016/j.neuron.2022.03.008> (2022).
35. Kenigsbuch, M. *et al.* A shared disease-associated oligodendrocyte signature among multiple CNS pathologies. *Nat. Neurosci.* **25**, 876–886. <https://doi.org/10.1038/s41593-022-01104-7> (2022).
36. Limantoro, J., de Liyis, B. G. & Sutedja, J. C. Akt signaling pathway: A potential therapy for Alzheimer's disease through glycogen synthase kinase 3 beta inhibition. *Egypt. J. Neurol. Psychiatry Neurosurg.* **59**, 147. <https://doi.org/10.1186/s41983-023-00751-2> (2023).
37. Wolf, F. A., Angerer, P. & Theis, F. J. SCANPY: Large-scale single-cell gene expression data analysis. *Genome Biol.* **19**, 15. <https://doi.org/10.1186/s13059-017-1382-0> (2018).
38. Polanski, K. *et al.* BBKNN: Fast batch alignment of single cell transcriptomes. *Bioinformatics* **36**, 964–965 (2020).
39. Aibar, S. *et al.* SCENIC: Single-cell regulatory network inference and clustering. *Nat. Methods* **14**, 1083–1086. <https://doi.org/10.1038/nmeth.4463> (2017).
40. Barbeira, A. N. *et al.* Exploring the phenotypic consequences of tissue specific gene expression variation inferred from GWAS summary statistics. *Nat. Commun.* **9**, 1825. <https://doi.org/10.1038/s41467-018-03621-1> (2018).
41. Zhang, M. J. *et al.* Polygenic enrichment distinguishes disease associations of individual cells in single-cell RNA-seq data. *Nat. Genet.* **54**, 1572–1580. <https://doi.org/10.1038/s41588-022-01167-z> (2022).
42. Chen, E. Y. *et al.* Enrichr: Interactive and collaborative HTML5 gene list enrichment analysis tool. *BMC Bioinform.* **14**, 128. <https://doi.org/10.1186/1471-2105-14-128> (2013).
43. Hänzelmann, S., Castelo, R. & Guinney, J. GSVA: Gene set variation analysis for microarray and RNA-seq data. *BMC Bioinform.* **14**, 7. <https://doi.org/10.1186/1471-2105-14-7> (2013).
44. Szklarczyk, D. *et al.* The STRING database in 2023: Protein-protein association networks and functional enrichment analyses for any sequenced genome of interest. *Nucleic Acids Res.* **51**, D638–d646. <https://doi.org/10.1093/nar/gkac1000> (2023).
45. Csardi, G. & Nepusz, T. The igraph software package for complex network research. *InterJ. Complex Syst.* **1695**, 1–9 (2006).
46. McInnes, L., Healy, J. & Melville, J. Umap: Uniform manifold approximation and projection for dimension reduction. *arXiv preprint arXiv:1802.03426* (2018).
47. Wingo, A. P. *et al.* Integrating human brain proteomes with genome-wide association data implicates new proteins in Alzheimer's disease pathogenesis. *Nat. Genet.* **53**, 143–146. <https://doi.org/10.1038/s41588-020-00773-z> (2021).
48. Xu, M. *et al.* Coexistence of multiple functional variants and genes underlies genetic risk locus 11p11.2 of Alzheimer's disease. *Biol. Psychiatry* **94**, 743–759. <https://doi.org/10.1016/j.biopsych.2023.05.020> (2023).
49. Holstege, H. *et al.* Exome sequencing identifies rare damaging variants in ATP8B4 and ABCA1 as risk factors for Alzheimer's disease. *Nat. Genet.* **54**, 1786–1794. <https://doi.org/10.1038/s41588-022-01208-7> (2022).
50. Sherva, R. *et al.* African ancestry GWAS of dementia in a large military cohort identifies significant risk loci. *Mol. Psychiatry* **28**, 1293–1302. <https://doi.org/10.1038/s41380-022-01890-3> (2023).
51. Jansen, I. E. *et al.* Genome-wide meta-analysis identifies new loci and functional pathways influencing Alzheimer's disease risk. *Nat. Genet.* **51**, 404–413. <https://doi.org/10.1038/s41588-018-0311-9> (2019).
52. Andrews, S. J., Fulton-Howard, B. & Goate, A. Interpretation of risk loci from genome-wide association studies of Alzheimer's disease. *Lancet Neurol.* **19**, 326–335. [https://doi.org/10.1016/s1474-4422\(19\)30435-1](https://doi.org/10.1016/s1474-4422(19)30435-1) (2020).
53. Fruman, D. A. *et al.* The PI3K pathway in human disease. *Cell* **170**, 605–635. <https://doi.org/10.1016/j.cell.2017.07.029> (2017).
54. Assinder, S. J., Dong, Q., Kovacevic, Z. & Richardson, D. R. The TGF- β , PI3K/Akt and PTEN pathways: Established and proposed biochemical integration in prostate cancer. *Biochem. J.* **417**, 411–421. <https://doi.org/10.1042/bj20081610> (2009).
55. Pini, L. *et al.* Brain atrophy in Alzheimer's disease and aging. *Ageing Res. Rev.* **30**, 25–48. <https://doi.org/10.1016/j.arr.2016.01.002> (2016).
56. Tietz, S. & Engelhardt, B. Brain barriers: Crosstalk between complex tight junctions and adherens junctions. *J. Cell Biol.* **209**, 493–506. <https://doi.org/10.1083/jcb.201412147> (2015).
57. Sun, X. *et al.* Enhanced interaction between focal adhesion and adherens junction proteins: Involvement in sphingosine 1-phosphate-induced endothelial barrier enhancement. *Microvasc. Res.* **77**, 304–313. <https://doi.org/10.1016/j.mvr.2008.12.004> (2009).
58. Del-Aguila, J. L. *et al.* A single-nuclei RNA sequencing study of Mendelian and sporadic AD in the human brain. *Alzheimers Res. Ther.* **11**, 71. <https://doi.org/10.1186/s13195-019-0524-x> (2019).

59. Mathys, H. *et al.* Single-cell transcriptomic analysis of Alzheimer's disease. *Nature* **570**, 332–337. <https://doi.org/10.1038/s41586-019-1195-2> (2019).
60. Grubman, A. *et al.* A single-cell atlas of entorhinal cortex from individuals with Alzheimer's disease reveals cell-type-specific gene expression regulation. *Nat. Neurosci.* **22**, 2087–2097. <https://doi.org/10.1038/s41593-019-0539-4> (2019).
61. Yang, A. C. *et al.* A human brain vascular atlas reveals diverse mediators of Alzheimer's risk. *Nature* **603**, 885–892. <https://doi.org/10.1038/s41586-021-04369-3> (2022).
62. Tsartsalis, S. *et al.* A single nuclear transcriptomic characterisation of mechanisms responsible for impaired angiogenesis and blood–brain barrier function in Alzheimer's disease. *Nat. Commun.* **15**, 2243. <https://doi.org/10.1038/s41467-024-46630-z> (2024).
63. Geirsdottir, L. *et al.* Cross-species single-cell analysis reveals divergence of the primate microglia program. *Cell* **179**, 1609–1622. <https://doi.org/10.1016/j.cell.2019.11.010> (2019).
64. Luquez, T. *et al.* Cell type-specific changes identified by single-cell transcriptomics in Alzheimer's disease. *Genome Med.* **14**, 136. <https://doi.org/10.1186/s13073-022-01136-5> (2022).
65. Murdock, M. H. & Tsai, L.-H. Insights into Alzheimer's disease from single-cell genomic approaches. *Nat. Neurosci.* **26**, 181–195. <https://doi.org/10.1038/s41593-022-01222-2> (2023).
66. İş, Ö. *et al.* Gliovascular transcriptional perturbations in Alzheimer's disease reveal molecular mechanisms of blood brain barrier dysfunction. *Nat. Commun.* **15**, 4758. <https://doi.org/10.1038/s41467-024-48926-6> (2024).
67. Meier-Stephenson, F. S. *et al.* Alzheimer's disease as an autoimmune disorder of innate immunity endogenously modulated by tryptophan metabolites. *Alzheimers Dementia* **8**, e12283. <https://doi.org/10.1002/trc2.12283> (2022).
68. Chen, X. *et al.* Microglia-mediated T cell infiltration drives neurodegeneration in tauopathy. *Nature* **615**, 668–677. <https://doi.org/10.1038/s41586-023-05788-0> (2023).
69. Orea-Soufi, A. *et al.* FOXO transcription factors as therapeutic targets in human diseases. *Trends Pharmacol. Sci.* **43**, 1070–1084. <https://doi.org/10.1016/j.tips.2022.09.010> (2022).
70. Bell, R. D. *et al.* Pericytes control key neurovascular functions and neuronal phenotype in the adult brain and during brain aging. *Neuron* **68**, 409–427. <https://doi.org/10.1016/j.neuron.2010.09.043> (2010).
71. Figueiredo, A. M. *et al.* Phosphoinositide 3-kinase-regulated pericyte maturation governs vascular remodeling. *Circulation* **142**, 688–704. <https://doi.org/10.1161/circulationaha.119.042354> (2020).
72. Nortley, R. *et al.* Amyloid β oligomers constrict human capillaries in Alzheimer's disease via signaling to pericytes. *Science* <https://doi.org/10.1126/science.aav9518> (2019).
73. Blumenthal, N. R., Hermanson, O., Heimrich, B. & Shastri, V. P. Stochastic nanoroughness modulates neuron–astrocyte interactions and function via mechanosensing cation channels. *Proc. Natl. Acad. Sci. USA* **111**, 16124–16129. <https://doi.org/10.1073/pnas.1412740111> (2014).
74. Sutherland, T. E., Dyer, D. P. & Allen, J. E. The extracellular matrix and the immune system: A mutually dependent relationship. *Science* **379**, eabp8964. <https://doi.org/10.1126/science.abp8964> (2023).
75. Drieu, A. *et al.* Parenchymal border macrophages regulate the flow dynamics of the cerebrospinal fluid. *Nature* **611**, 585–593. <https://doi.org/10.1038/s41586-022-05397-3> (2022).
76. Reed, M. J. *et al.* Increased hyaluronan and TSG-6 in association with neuropathologic changes of Alzheimer's disease. *J. Alzheimers Dis.* **67**, 91–102. <https://doi.org/10.3233/jad-180797> (2019).
77. Lorente-Gea, L. *et al.* Heparan sulfate proteoglycans undergo differential expression alterations in Alzheimer disease brains. *J. Neuropathol. Exp. Neurol.* **79**, 474–483. <https://doi.org/10.1093/jnen/nlaa016> (2020).
78. Goetzl, E. J. *et al.* Deficient neurotrophic factors of CSPG4-type neural cell exosomes in Alzheimer disease. *FASEB J.* **33**, 231–238. <https://doi.org/10.1096/fj.201801001> (2019).
79. Alata, W., Ye, Y., St-Amour, I., Vandal, M. & Calon, F. Human apolipoprotein E ϵ 4 expression impairs cerebral vascularization and blood–brain barrier function in mice. *J. Cereb. Blood Flow Metab.* **35**, 86–94. <https://doi.org/10.1038/jcbfm.2014.172> (2015).

Acknowledgements

Thanks to all authors for their efforts and financial support. Thanks to the original author for sharing the data.

Author contributions

Changhe Shi and Yuming Xu conceptualized the project. Mengjie Li and Xiaoyan Hao designed, performed, and analyzed the data. They also wrote the initial draft of the manuscript with input from all co-authors. Zhengwei Hu, Jingjing Shi, Dongrui Ma, Dongrui Ma, Shuangjie Li, Chunyan Zuo, and Yuanyuan Liang were responsible for data analysis and visualization. Mibo Tang and Jie Tian reviewed the manuscript. Changhe Shi, Yuming Xu, and Chengyuan Mao edited the final version of the manuscript. Changhe Shi, Chengyuan Mao, and Jie Tian secured the necessary funding.

Funding

This work was supported by the National Natural Science Foundation of China to C.S. [Grant Number 82171247, 81974211], and Funding for Scientific Research and Innovation Team of the First Affiliated Hospital of Zhengzhou University to C.S. [Grant Number ZYCXTD2023011], the Scientific and Technological Research Projects in Henan province to Dr. Jie Tian [Grant Number 222102310033], the National Natural Science Foundation of China to C.M. [Grant Number 82271277].

Competing interests

The authors declare no competing interests.

Additional information

Supplementary Information The online version contains supplementary material available at <https://doi.org/10.1038/s41598-024-71888-0>.

Correspondence and requests for materials should be addressed to C.S.

Reprints and permissions information is available at www.nature.com/reprints.

Publisher's note Springer Nature remains neutral with regard to jurisdictional claims in published maps and institutional affiliations.

Open Access This article is licensed under a Creative Commons Attribution-NonCommercial-NoDerivatives 4.0 International License, which permits any non-commercial use, sharing, distribution and reproduction in any medium or format, as long as you give appropriate credit to the original author(s) and the source, provide a link to the Creative Commons licence, and indicate if you modified the licensed material. You do not have permission under this licence to share adapted material derived from this article or parts of it. The images or other third party material in this article are included in the article's Creative Commons licence, unless indicated otherwise in a credit line to the material. If material is not included in the article's Creative Commons licence and your intended use is not permitted by statutory regulation or exceeds the permitted use, you will need to obtain permission directly from the copyright holder. To view a copy of this licence, visit <http://creativecommons.org/licenses/by-nc-nd/4.0/>.

© The Author(s) 2024